Semiconductor–half metal transition at the $Fe_3O_4(001)$ surface upon hydrogen adsorption

Gareth S. Parkinson,[1,2] Narasimham Mulakaluri,[3,4] Yaroslav Losovyj,[5] Peter Jacobson,[1,2]
Rossitza Pentcheva,[3] and Ulrike Diebold[1,2,*]

[1]*Department of Physics, Tulane University, New Orleans, Louisiana 70118, USA*
[2]*Institute of Applied Physics, Vienna University of Technology, Vienna, Austria*
[3]*Department of Earth and Environmental Sciences, University of Munich, Theresienstr. 41, 80333 Munich, Germany*
[4]*Fritz-Haber-Institut der Max-Planck-Gesellschaft, Faradayweg 4-6, D-14195 Berlin, Germany*
[5]*Center for Advanced Microstructures and Devices, Louisiana State University, 6980 Jefferson Highway, Baton Rouge, Louisiana 70806, USA*

(Received 8 June 2010; revised manuscript received 13 August 2010; published 9 September 2010)

The adsorption of H on the magnetite (001) surface was studied with photoemission spectroscopies, scanning tunneling microscopy, and density-functional theory. At saturation coverage the insulating $(\sqrt{2}\times\sqrt{2})R45°$ reconstruction is lifted and the surface undergoes a semiconductor–half metal transition. This transition involves subtle changes in the local geometric structure linked to an enrichment of Fe^{2+} cations at the surface. The ability to manipulate the electronic properties by surface engineering has important implications for magnetite-based spintronic devices.

DOI: 10.1103/PhysRevB.82.125413 PACS number(s): 68.37.Ef, 68.43.Bc, 68.47.Gh, 73.20.−r

I. INTRODUCTION

The Earth's oldest permanent magnet, magnetite (Fe_3O_4), continues to attract attention due to its fascinating properties. The predicted half metallicity in the room-temperature (RT) cubic phase[1] has led to significant interest in utilizing magnetite in spintronics applications. The fact that magnetite exhibits a high Curie temperature (858 K) and similar conductivity to many semiconductors makes it particularly attractive as an electrode in devices such as magnetic tunnel junctions. However, experimental verification of the half metallicity has proven problematic. Experiments using spin-polarized photoemission have measured varying degrees of spin polarization at the Fermi level (40–80 %) (Refs. 2–5) for the bulk material, in contrast to the density-functional theory (DFT) prediction of 100% for the bulk (RT) phase.[1] However, photoemission is essentially a surface-sensitive technique that can only be reliably applied to measurements of bulk electronic structure in the absence of strong surface effects, even for high-energy photons.[6] The surface electronic structure of magnetite (001), however, differs from the bulk. A small band gap of 0.2–0.3 eV is opened by the presence of an interesting surface reconstruction.[7–11] The novel $(\sqrt{2}\times\sqrt{2})R45°$ surface reconstruction, where the surface unit cell is enlarged and rotated by 45° with respect to the ideal bulk termination, was detailed in a prior publication.[7]

Here we utilize surface science techniques combined with DFT calculations to study the adsorption of atomic H on the reconstructed $Fe_3O_4(001)$ surface. At saturation coverage H lifts the insulating $(\sqrt{2}\times\sqrt{2})R45°$ reconstruction and generates Fe^{2+} in the surface layer producing a half-metallic surface with structure close to the ideal (1×1) bulk termination.

II. EXPERIMENTAL AND COMPUTATIONAL DETAILS

The scanning tunneling microscopy (STM), low-energy electron diffraction (LEED), ultraviolet (UPS), and x-ray photoelectron spectroscopy (XPS) data were acquired in ultrahigh vacuum with a base pressure of 10^{-10} mbar. All STM images were taken in the constant-current mode imaging empty states (V_{sample}=+0.7 to +1.8 V and I_{tunnel} =0.15–0.3 nA) at room temperature. The surface was exposed to hydrogen by backfilling the chamber with H_2 while keeping a hot W filament in line-of-sight with the sample. UPS was performed on the NIM beamline at the Center for Advanced Microstructures and Devices (CAMD) in Baton Rouge, LA. Angular mode data were collected with energy resolution set to ~20 meV using 29 eV photons with a 45° incident angle and normal-emission geometry. Energy distribution curves were acquired from data integrated in ±2° angle around the surface normal. A natural $Fe_3O_4(001)$ crystal (Commercial Crystal Laboratories) was prepared by cycles of sputtering (1 keV, 5 μA, 10 min) and annealing (820 K, 10 min) until a sharp $(\sqrt{2}\times\sqrt{2})R45°$ LEED pattern was observed. To prevent reduction in the surface, annealing in 10^{-6} mbar O_2 at 820 K for 5 min was performed during each cleaning cycle. X-ray photoelectron spectroscopy (XPS) showed no sign of contamination other than 4 at. % Si that is present in the mineral sample. The surface Si is easily identified in STM (not shown) and can be avoided during the imaging. DFT calculations were performed with the WIEN2K code.[12] Electronic correlations beyond the generalized gradient approximation[13] are taken into account by an additional on-site Coulomb repulsion term (LDA/GGA +U) (Ref. 14) with U=5 eV and J=1 eV, similar to values used for bulk Fe_3O_4.[15,16] For further details see Ref. 8. The surface is modeled by a supercell consisting of seven B and six A layers [containing tetrahedral Fe(A)] with H adsorbed on both sides of the slab. All coordinates of the adsorbates and the outer two BA layers are fully relaxed.

III. RESULTS AND DISCUSSION

Figure 1(a) shows the clean $Fe_3O_4(001)$ surface as determined previously.[7,10] The blue (dark gray) and gold (light

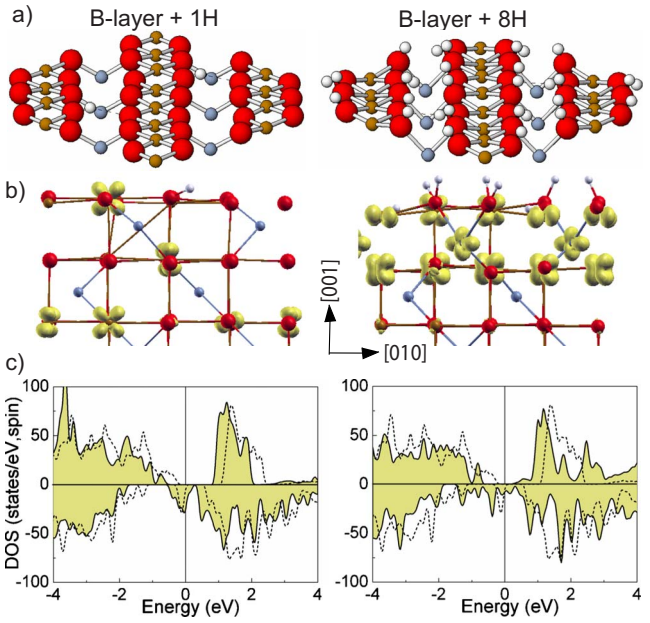

FIG. 1. (Color online) Modification of an $Fe_3O_4(001)$ surface with (left) 1 and (right) 8 Hydrogen atoms per surface unit cell. O atoms are red/large, Fe(B) are gold/gray and Fe(A) are blue/light gray. (a) Adsorption geometry. (b) Side view showing the occupation of the minority t_{2g} orbitals at the Fe(B) sites (i.e., ions with Fe^{2+} character); electron density integrated between −1.3 eV and E_F. (c) Total density of states (solid black line with yellow filled area) showing the characteristics of half-metallic system. For comparison the DOS of the clean surface (modified B layer; black dashed line), shows a band gap of 0.3 eV.

gray) spheres represent the Fe(A) and Fe(B) atoms that, in the bulk, are in a tetrahedral and octahedral coordination, respectively. A lattice distortion results in pairs of Fe(B) atoms relaxing perpendicular to the [110] row; this distortion induces a small band gap at the surface,[8,11] see also the dashed curves in Fig. 1(c). For a single adsorbed H atom, we find preferential adsorption at surface oxygen without a subsurface Fe(A) [Fig. 1(a), left]. The adsorbate is strongly displaced laterally from the atop position and the OH group is nearly parallel to the surface [Fig. 1(b), left], leading to the formation of an H bond (2.24 Å) with the neighboring surface O. In the case of full hydroxylation (Fig. 1, right) H adatoms are found in similar tilted atop configurations. The strong lateral relaxations at the reconstructed clean surface [these can be as much as 0.36 Å (Refs. 7 and 10)] are significantly reduced upon saturation with atomic H to less than 0.05 Å from the bulk positions.

Figure 1(b) shows the occupation of the sixth orbital of Fe(B), i.e., only the positions with Fe^{2+} character have a nonvanishing electron density. Whereas the clean[8,11] and water adsorbed[8] $Fe_3O_4(001)$ surfaces have exclusively Fe^{3+} in the surface layer, H adsorption leads to reduction to Fe^{2+}. At saturation of the surface oxygen sites (B-layer +8H) both the surface and subsurface B layers are completely switched to Fe^{2+}; the tetrahedrally coordinated Fe atoms in the subsurface A layer are also converted to Fe^{2+}. A consequence of the enhanced Fe^{2+} concentration is that the Fe(B)-O in-plane bond lengths increase to 2.08–2.14 Å.

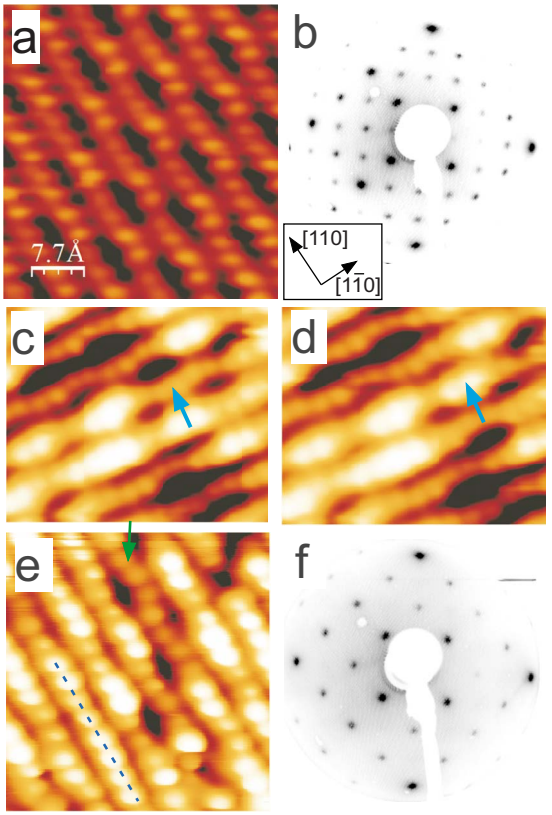

FIG. 2. (Color online) The clean $Fe_3O_4(001)$ $(\sqrt{2}\times\sqrt{2})R45°$ surface: (a) STM image (V_{sample}=+1.7 V, I_{tunnel}=0.14 nA) and (b) LEED pattern (E_{el}=90 eV). (c) and (d) Consecutive STM images ($\Theta_H\sim$0.07 ML, 4 nm×3.5 nm, 1.4 V, 0.14 nA) at low atomic H coverage. The arrows mark the motion of a H-induced bright double protrusion to a neighboring row. (e) STM image ($\Theta_H\sim$0.25 ML, 4×4 nm^2, 0.76 V, 0.21 nA). One row of Fe(B) atoms is bright and straight (dashed blue line), an uncovered section, marked by the green arrow, displays the characteristic Fe(B) "wiggle." (f) LEED pattern from the H saturated surface displaying (1×1) symmetry.

Figure 1(c) shows the total DOS for the H adsorbed surfaces. The clean surface (dashed line) shows a band gap of 0.3 eV as observed previously.[8,11] Adsorption of H leads to Fe^{2+} in the surface layer with an occupied t_{2g} orbital in the minority (spin-down) channel. This orbital leads to an enhanced density of states (DOS) at and below the Fermi level, and a semiconductor–half metal transition for $H/Fe_3O_4(001)$. In addition, the charge and orbital ordering of the deeper layers is affected by the hydrogen adsorption.

To complement the DFT results, we have performed experiments on a $Fe_3O_4(001)$ sample with varying coverages of atomic H. Empty states STM images of the clean surface [Fig. 2(a)] show the characteristic undulating Fe(B) rows of the $(\sqrt{2}\times\sqrt{2})R45°$ reconstruction along the [110] direction;[4,17–19] a LEED pattern obtained from the same surface is shown in Fig. 2(b).

Two consecutive STM images recorded over the same sample area following 3 min H exposure (H_2 pressure of 10^{-7} mbar) are shown in Figs. 2(c) and 2(d). Several bright double protrusions situated at Fe(B) sites are observed. This suggests that the adsorbed H atom is not directly imaged, rather that the neighboring Fe cations (which DFT suggests

are converted to Fe^{2+}) have a higher contrast than those on the clean surface. This assignment is strengthened by the observation that the double protrusions frequently jump to the opposite Fe(B) row and back again at room temperature, an example of such a jump is indicated by the arrows in Figs. 2(c) and 2(d). This can be explained by hopping of the H atom to the symmetrically equivalent O site within the unit cell [see Fig. 1(a)], causing the Fe(B) atoms on the opposite row to be imaged bright. The DFT predicted geometry and H bonding are consistent with facile hydrogen hopping at room temperature.

As the exposure to H atoms (Θ_H) is increased the density of the bright Fe(B) atoms increases. At $\Theta_H \sim 0.25$ ML [1 ML=1/2 the Fe(B) density] many areas show a local ordering, with double protrusions spaced according to the $(\sqrt{2}\times\sqrt{2})R45°$ reconstruction (data not shown). Figure 2(e) shows the surface after 30 min of H exposure [$p(H_2) = 10^{-7}$ mbar]. Now only a small section of the clean Fe(B) row is visible (green arrow). Also evident are straight rows of bright protrusions, indicated by the dashed blue line. The straightening of the Fe(B) rows is consistent with the DFT prediction that the surface atoms relax back to bulk-terminated positions following H adsorption. Upon saturation coverage of atomic H (30 min, 10^{-6} mbar) the surface exhibits (1×1) symmetry in LEED [Fig. 2(f)], suggesting that the $(\sqrt{2}\times\sqrt{2})R45°$ reconstruction is completely lifted. The $(\sqrt{2}\times\sqrt{2})R45°$ LEED pattern is recovered only after annealing the sample to ~623 K (data not shown), presumably as H leaves the surface.

In addition to structural modifications, the DFT results suggest that adsorption of atomic H strongly affects the electronic structure of the $Fe_3O_4(001)$ surface. Figure 3(a) shows UPS data of the reconstructed clean surface and alongside data acquired from the H saturated surface. The position of the chemical potential was calibrated by the Fermi edge (E_F) of the molybdenum sample plate, in contact with the magnetite crystal. Normal-emission spectra from the clean surface show states at binding energies of ~0.6, 2.8, 4, and 6 eV, in good agreement with previous results,[6,20] although the features at 4 and 6 eV are generally not resolved and commonly appear as a single broad feature centered at ~5.5 eV. It is important to note that the clean-surface photoemission data inevitably represent a superposition of photons emerging from both the $(\sqrt{2}\times\sqrt{2})R45°$ surface and the immediate subsurface layers. Since the surface layer contains only Fe^{3+} cations,[8,11] the intensity observed at 0.6 eV can be attributed to Fe^{2+} cations[8,11] in the subsurface. Saturation with H causes a dramatic increase in spectral weight distribution near the Fermi level and the Fermi edge is significantly enhanced. The inset in Fig. 3(a) shows the region close to E_F along with a scaled reference spectrum collected for the molybdenum sample plate (blue) indicating the metallic nature of the H-adsorbed surface. In Fe_3O_4, features near E_F originate from $3d$-$3d$ transitions at the Fe(B) ions with Fe^{2+} character,[21,22] therefore the data suggest that surface Fe(B) atoms have been converted to Fe^{2+} by the adsorption of atomic H.

The oxidation state of near-surface Fe atoms of $Fe_3O_4(001)$ before and after H exposure was probed by monitoring the Fe $2p$ region with XPS [Fig. 3(b)] in a grazing exit configuration. For magnetite, which contains Fe^{2+} and Fe^{3+} cations in the bulk, broad Fe $2p$ peaks are observed at 709 eV (Fe^{2+}) and 711.4 eV (Fe^{3+}) plus several peaks attributable to satellite peaks at higher binding energies.[23] While the complicated nature of the Fe $2p$ spectra makes quantitative analysis difficult, there is a clear shoulder present at 709 eV, consistent with an increase in Fe^{2+} cations. We conclude that the H-dosed surface region has an increased proportion of Fe^{2+} cations relative to the clean surface. Complementary O $1s$ XPS spectra (not shown) exhibit a shoulder on the high binding energy side (~532 eV) consistent with hydroxyl groups. No shift is observed in the position of the O $1s$ signal from the subsurface O atoms.

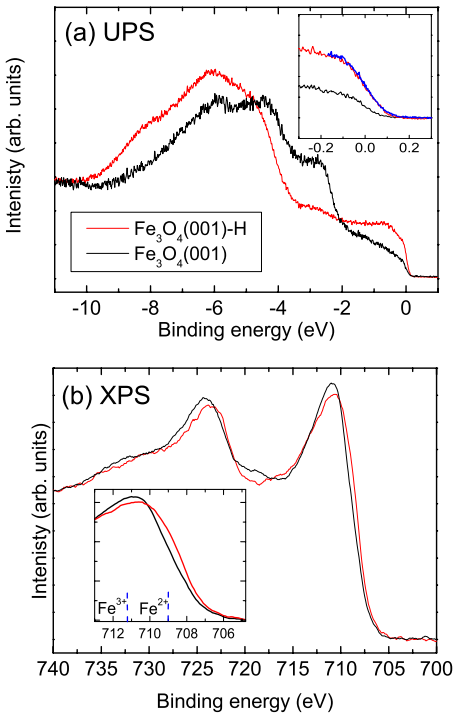

FIG. 3. (Color online) (a) UPS spectra ($h\nu$=29 eV, normal emission) from the clean (black) and H-covered (red/gray) $Fe_3O_4(001)$ surfaces. The inset shows the region around E_F; the blue line shows the metallic Fermi edge acquired from the molybdenum sample plate. (b) Fe $2p$ XPS spectra (Al $K\alpha$ photons, emission angle at 60° from normal) from the clean (black) and H-covered (red) $Fe_3O_4(001)$ surfaces. The inset magnifies the shift in the leading edge of the Fe $2p_{3/2}$ peak to lower binding energy and indicates the expected position for Fe^{2+} and Fe^{3+} cations.

These results clearly demonstrate that H adsorption on $Fe_3O_4(001)$ lifts the $(\sqrt{2}\times\sqrt{2})R45°$ surface reconstruction and induces a semiconductor–half metal transition in the surface region. It is interesting to note that these changes to the structure and electronic properties are exactly those expected if the surface were to undergo the Verwey transition, as the bulk material does at 123 K.[24,25] However, the DFT calculations, UPS and XPS data presented here indicate that the H saturated surface contains Fe^{2+} ions, creating a half-metallic interface that is distinct from the bulk conducting phase, where hopping of electrons between Fe^{3+} and Fe^{2+} ions on the Fe(B) sublattice is proposed.[24,25] On the other hand, partial hydrogenation, with no H at the energetically disfavored

position next to tetrahedral irons, leads to a surface with Fe^{3+} and Fe^{2+} and may allow for electron hopping.

That the $Fe_3O_4(001)$ surface can undergo a semiconductor–half metal transition through adsorption of atomic H provides an opportunity to solve ambiguities surrounding fundamental properties of magnetite.[6] Recent spin-resolved photoemission studies have found less than the expected 100% spin polarization at the Fermi level but there has been discussion of the extent to which the surface reconstruction of $Fe_3O_4(001)$ may cause spin flipping as the spin-polarized photoelectrons are transmitted into vacuum.[3–5] Lifting of the surface reconstruction as demonstrated in this work should help unambiguously resolve this critical issue.

Recent studies have highlighted the importance of interface effects to the performance of ferromagnet-based spintronic devices such as magnetic tunnel junctions (see, for example, Ref. 26) In particular, devices based on magnetite electrodes have demonstrated disappointing performance, with the authors often citing the influence of interface effects on the transport properties (see, for example, Refs. 27 and 28). Here we demonstrate using a simple, tractable model system that properties related to magnetotransport at magnetite interfaces can be manipulated by surface engineering. This can be used as a basis for understanding more complicated, technologically relevant interfaces formed with semiconductors. We propose that $Fe_3O_4(001)$ adsorption studies with the high-mobility organic semiconductors such as alq3, rubrene, and pentacene, which have been shown to facilitate spin-polarized transport over tens of nanometers,[29] represent an exciting avenue for future study.

Finally, while water adsorption and dissociation does not change the valence state of Fe in the surface layer,[8] here we find that H adsorption enriches the surface with Fe^{2+}. This provides a path to engineer the reactivity of $Fe_3O_4(001)$ in catalitic and geological environments. A recent paper by Skomurski *et al.*[30] shows clearly that the availability of Fe^{2+} at the $Fe_3O_4(001)$ is directly related to rate of redox reactions.

IV. SUMMARY

Based on STM and LEED measurements and DFT calculations, we have demonstrated that the $(\sqrt{2}\times\sqrt{2})R45°$ surface reconstruction of $Fe_3O_4(001)$ is lifted upon adsorption of atomic H at room temperature, leading to a surface with (1×1) symmetry. Valence-band photoemission data clearly show that the structural change is accompanied by a semiconductor–metal transition at the surface. DFT calculations demonstrate that the modified surface possesses only spin-down electrons at the Fermi level and therefore a half-metallic interface is produced. The ability to tailor the interface properties has exciting implications for the use of magnetite in technology.

While this paper was in review we became aware of work published about the same system by Kurahashi *et al.*[31] The authors used a spin-polarized metastable helium-atom beam to show that the spin polarization at the $Fe_3O_4(001)$ surface is recovered by saturation coverage with atomic H, in accord with the theoretical and experimental results described here.

ACKNOWLEDGMENTS

This work was supported by the Board of Regents of the State of Louisiana [Contract No. LEQSF (2007–10)-RD-B-08], the National Science Foundation (Grant No. CHE-0715576), and the German Science Foundation (Grant No. PE883/1-2). We acknowledge computational time at the Leibniz Rechenzentrum, Garching.

*diebold@iap.tuwien.ac.at

[1] Z. Zhang and S. Satpathy, Phys. Rev. B **44**, 13319 (1991).
[2] S. A. Morton, G. D. Waddill, S. Kim, I. K. Schuller, S. A. Chambers, and J. G. Tobin, Surf. Sci. **513**, L451 (2002).
[3] J. G. Tobin, S. A. Morton, S. W. Yu, G. D. Waddill, I. K. Schuller, and S. A. Chambers, J. Phys.: Condens. Matter **19**, 315218 (2007).
[4] M. Fonin, R. Pentcheva, Y. S. Dedkov, M. Sperlich, D. V. Vyalikh, M. Scheffler, U. Rudiger, and G. Guntherodt, Phys. Rev. B **72**, 104436 (2005).
[5] M. Fonin, Y. S. Dedkov, R. Pentcheva, U. Rüdiger, and G. Güntherodt, J. Phys.: Condens. Matter **19**, 315217 (2007).
[6] D. Schrupp, M. Sing, M. Tsunekawa, H. Fujiwara, S. Kasai, A. Sekiyama, S. Suga, T. Muro, V. A. M. Brabers, and R. Claessen, Europhys. Lett. **70**, 789 (2005).
[7] R. Pentcheva, F. Wendler, H. L. Meyerheim, W. Moritz, N. Jedrecy, and M. Scheffler, Phys. Rev. Lett. **94**, 126101 (2005).
[8] N. Mulakaluri, R. Pentcheva, M. Wieland, W. Moritz, and M. Scheffler, Phys. Rev. Lett. **103**, 176102 (2009).
[9] K. Jordan, A. Cazacu, G. Manai, S. F. Ceballos, S. Murphy, and I. V. Shvets, Phys. Rev. B **74**, 085416 (2006).
[10] R. Pentcheva, W. Moritz, J. Rundgren, S. Frank, D. Schrupp, and M. Scheffler, Surf. Sci. **602**, 1299 (2008).
[11] Z. Łodziana, Phys. Rev. Lett. **99**, 206402 (2007).
[12] P. Blaha, K. Schwarz, G. Madsen, D. Kvasnicka, and J. Luitz, *WIEN2k, An Augmented Plane Wave Plus Orbitals Program for Calculating Crystal Properties*, edited by K. Schwarz (Technische Universität Wien, Austria, 2001).
[13] J. P. Perdew, K. Burke, and M. Ernzerhof, Phys. Rev. Lett. **77**, 3865 (1996).
[14] V. I. Anisimov, I. V. Solovyev, M. A. Korotin, M. T. Czyżyk, and G. A. Sawatzky, Phys. Rev. B **48**, 16929 (1993).
[15] I. Leonov, A. N. Yaresko, V. N. Antonov, M. A. Korotin, and V. I. Anisimov, Phys. Rev. Lett. **93**, 146404 (2004).
[16] H.-T. Jeng, G. Y. Guo, and D. J. Huang, Phys. Rev. Lett. **93**, 156403 (2004).
[17] N. Spiridis, J. Barbasz, Z. Lodziana, and J. Korecki, Phys. Rev. B **74**, 155423 (2006).
[18] B. Stanka, W. Hebenstreit, U. Diebold, and S. A. Chambers, Surf. Sci. **448**, 49 (2000).
[19] S. F. Ceballos, G. Mariotto, K. Jordan, S. Murphy, C. Seoighe, and I. V. Shvets, Surf. Sci. **548**, 106 (2004).
[20] R. Zalecki, A. Kolodziejczyk, J. Korecki, N. Spiridis, M. Zajac, A. Kozlowski, Z. Kakol, and D. Antolak, Phys. Status Solidi B

243, 103 (2006).
[21] V. I. Anisimov, I. S. Elfimov, N. Hamada, and K. Terakura, Phys. Rev. B **54**, 4387 (1996).
[22] A. Yanase and N. I. Hamada, J. Phys. Soc. Jpn. **68**, 1607 (1999).
[23] A. P. Grosvenor, B. A. Kobe, M. C. Biesinger, and N. S. McIntyre, Surf. Interface Anal. **36**, 1564 (2004).
[24] E. J. W. Verwey, Nature (London) **144**, 327 (1939).
[25] F. Walz, J. Phys.: Condens. Matter **14**, R285 (2002).
[26] S. K. Arora, H. C. Wu, R. J. Choudhary, I. V. Shvets, O. N. Mryasov, H. Z. Yao, and W. Y. Ching, Phys. Rev. B **77**, 134443 (2008).
[27] B. B. Nelson-Cheeseman, R. V. Chopdekar, L. M. B. Alldredge, J. S. Bettinger, E. Arenholz, and Y. Suzuki, Phys. Rev. B **76**, 220410 (2007).
[28] R. Arras, L. Calmels, and B. Warot-Fonrose, IEEE Trans. Magn. **46**, 1730 (2010).
[29] A. R. Rocha, V. M. Garcia-Suarez, S. W. Bailey, C. J. Lambert, J. Ferrer, and S. Sanvito, Nature Mater. **4**, 335 (2005).
[30] F. M. Skomurski, S. Kerisit, and K. M. Rosso, Geochim. Cosmochim. Acta **74**, 4234 (2010).
[31] M. Kurahashi, X. Sun, and Y. Yamauchi, Phys. Rev. B **81**, 193402 (2010).